Materials Research Bulletin 47 (2012) 1604–1608

Contents lists available at SciVerse ScienceDirect

Materials Research Bulletin

journal homepage: www.elsevier.com/locate/matresbu

Short communication

Transformation from hollow carbon octahedra to compressed octahedra and their use in lithium-ion batteries

Tao Mei [a], Na Li [a], Qianwen Li [a], Zheng Xing [a], Kaibin Tang [a], Yongchun Zhu [a,*], Yitai Qian [a,b,*], Xiaoyan Shen [c]

[a] Hefei National Laboratory for Physical Science at Microscale and Department of Chemistry, University of Science and Technology of China, Hefei, Anhui 230026, PR China
[b] School of Chemistry and Chemical Engineering, Shandong University, Jinan 250100, PR China
[c] Jiangsu Highstar Battery Manufacturing CO., LTD, PR China

ARTICLE INFO

Article history:
Received 29 August 2011
Received in revised form 23 November 2011
Accepted 1 March 2012
Available online 10 March 2012

Keywords:
A. Nanostructure
B. Chemical synthesis
C. Electrochemical properties
C. Raman spectroscopy
C. X-ray diffraction

ABSTRACT

Hollow carbon octahedra with an average size of 300 nm and a shell thickness of 2.5 nm were prepared by a reaction starting from ferrocene and $Mg(CH_3COO)_2 \cdot 4H_2O$ at 700 °C for 10 h. They became compressed and turned into deflated balloon-like octahedra when the reaction time was increased to 16 h. It was proposed that the gas pressure generated during the reaction process induced the transformation from broken carbon hollow octahedra into deflated balloon-like compressed octahedra. X-ray powder diffraction and Raman spectroscopy indicate that the as-obtained carbon products possess a graphitic structure and high-resolution transmission electron microscopy images indicate that they have low crystallinity. Their application as an electrode shows reversible capacity of 353 mAh g^{-1} after 100 cycles in the charge/discharge experiments of secondary lithium ion batteries.

1. Introduction

Carbon materials have been used as electrodes for lithium-ion batteries. Due to nanoscale carbon materials usually possess large surface areas and present a relatively large number of lithium-ion insertion sites on their surface, charge-transfer resistances at the interface between the electrolyte and active electrode materials are expected to be small. In addition, the carbon nanostructure makes it possible to shorten the diffusion paths, resulting in the apparent fast diffusion of lithium-ion [1]. Recently, carbon nanomaterials with various morphologies have been intensively studied as negative electrode materials in lithium-ion batteries. Some carbon nanomaterials have been reported to exhibit good electrochemical properties. For example, flower-like carbon nanosheet aggregations were produced by a solvothermal technique at 800 °C, which exhibited a reversible capacity of 380 mAh g^{-1} after 30 cycles at the current density of 100 mA g^{-1} [2]. Carbon spheres prepared by thermal decomposition, possessed a storage capacity of ~300 mAh g^{-1} after 135 cycles with a current density of 0.2 mA cm^{-2} [3].

As reported, the unique hollow structure could facilitate Li^+ transport by offering a short diffusion distance and a large surface area [4]. In addition, since the hollow carbon structures could serve as barriers to suppress agglomeration of active particles and provide space for buffering volume expansion, hollow carbon structures are sometimes used to address the capacity-fading problem of other anode materials with huge volume changes during the Li insertion and extraction [5,6]. For hollow carbon structures, they have attracted comprehensive research interest owing to their potential applications in lithium-ion batteries [7–9]. Interconnected hollow structured carbon materials exhibit a reversible capacity as 630 mAh g^{-1} after 50 cycles at a rate of C/10 [10]. Hollow carbon nanofibers/graphene hybrid material showed high reversible capacity above 600 mAh g^{-1} after 30 cycles at a current density of 0.12 mA cm^{-2} [11]. Graphene-constructed hollow carbon spheres presented a stable reversible capacity as 600 mAh g^{-1} after 30 cycles at a rate of C/5 [12]. The hollow carbon nanofibers showed capacity of ~220 mAh g^{-1} up to 30 cycles under a current density as 0.1 mA cm^{-2} [1].

Nowadays, different methods have been used to synthesize hollow carbon structures. Templating against colloidal particles is probably the most effective and general method for preparing hollow carbon structures [13–15]. In recent years, some hollow carbon materials, such as mesoporous carbon [16], nanocages [17], nanotubes [18], capsules [19] and polyhedrons [20] have been prepared by in situ template method. For instance, hollow

---

* Corresponding authors at: Hefei National Laboratory for Physical Science at Microscale and Department of Chemistry, University of Science and Technology of China, Hefei, Anhui 230026, PR China. Tel.: +86 551 3607402; fax: +86 551 3607402.
E-mail address: ytqian@ustc.edu.cn (Y. Qian).

0025-5408/$ – see front matter © 2012 Elsevier Ltd. All rights reserved.
doi:10.1016/j.materresbull.2012.03.011

hexapod-like carbon materials and bundles of carbon nanotubes were obtained by C_2H_5OH-$Fe(C_5H_5)_2$, using generated Fe_3O_4 as in situ template at 600 and 800 °C, respectively [21].

In this study, we demonstrate the in situ template route to synthesize hollow carbon octahedra (HCOs). Appropriate extending the reaction time will realize the morphology transformation from HCOs to deflated balloon-like compressed HCOs. The as-obtained hollow structures demonstrate stable reversible capacity about 353 mAh g^{-1} after 100 cycles.

2. Experimental

2.1. Preparation of HCOs

All the chemical reagents used here were analytical grade without further purification. In a typical synthesis process, 0.5 g ferrocene and 2.0 g $Mg(CH_3COO)_2·4H_2O$ were mixed and placed in a stainless-steel autoclave of 20 mL capacity. The autoclave was sealed and put into an electronic furnace from room temperature with an increasing speed of 10 °C/min to 700 °C then maintained at 700 °C for 10 h, after that it was cooled to room temperature naturally. In order to remove the byproducts, the precipitates in the autoclave were collected and washed by dilute hydrochloric acid, absolute ethanol, and distilled water several times. After that, the products were dried in a vacuum at 60 °C for 5 h for further characterization.

2.2. Preparation of deflated balloon-like compressed HCOs

The deflated balloon-like compressed HCOs were obtained under the same conditions except for extending the reaction time to 16 h.

2.3. Characterization

X-ray powder diffraction (XRD) patterns of the products were recorded on a Philips X'pert X-ray diffractometer with Cu Ka radiation (k = 1.54182 Å). The microstructure was observed on a transmission electron microscope (TEM, H7650), a high-resolution transmission electron microscope (HRTEM, JEOL-2010) with an accelerating voltage of 200 kV, the selected area electron diffraction (SAED) and a field-emitting scanning electron microscope (SEM, JEOL-JSM-6700F). Raman spectrum was carried out on a JY LABRAM-HR confocal laser micro-Raman spectrometer using Ar^+ laser excitation with a wavelength of 514.5 nm. X-ray photoelectron spectra (XPS) were recorded on a VGESCA-LAB MKII X-ray photoelectron spectrometer, using non-monochromated Mg Kα X-ray radiation as the excitation source.

Charge/discharge tests were carried out using coin-type cells (size: 2016), which consisted of an active material working electrode and a Li foil counter electrode separated by a Celgard 2300 microporous membrane. To prepare the working electrode, active material and polyvinylidene fluoride were mixed by the weight ratio of 9:1 with N-methyl pyrrolidone serving as the solvent to obtain the slurry. After coating the slurry onto a copper mesh current collector, the electrode was dried at 120 °C in vacuum for 12 h. Typical loadings of the electrodes were between 4 and 5 mg of active material. 1 mol/L solution of $LiPF_6$ dissolved in ethylene carbonate/dimethyl carbonate (1:1 volume ratio) was used as the electrolyte. The cells were assembled in an argon-filled glove box (Mikrouna, Super 1220/750/900, China) and then charged/discharged galvanostatically from 3.0 to 0.01 V versus Li^+/Li at current densities of 200 mA g^{-1}.

3. Results and discussion

Fig. 1a shows the typical XRD pattern of the raw sample before washed by dilute hydrochloric acid. The diffraction peak (marked with *) can be readily indexed to hexagonal graphite (JCPDS Card, No. 41-1487). The other diffraction peaks were indexed as crystalline face-centered cubic (fcc) Fe_3O_4 (JCPDS Card, No. 19-0629). Fig. 1b shows the XRD pattern of the as-obtained sample after the acid treatment. The distinct diffraction peaks with d-spacing of 3.375 and 2.039 Å can be indexed as the diffraction of (0 0 2) and (1 0 1) from hexagonal graphite (JCPDS card No. 41-1487).

The representative Raman spectrum of the above sample (Fig. 2) shows two obvious peaks at 1358 and 1585 cm^{-1} which correspond to the D-band and G-bond of graphite. The peak at 1585 cm^{-1}, named G-band, corresponds to an E_{2g} vibration mode of graphite and is related to the vibration of sp^2-bonded carbon atoms in a 2D hexagonal lattice. The peak at 1358 cm^{-1}, named D-band, is associated with the vibration of carbon atoms with dangling bonds in-plane terminations of disordered graphite [22]. The ID/IG value of the sample is 0.94, which indicates that the as-obtained sample possesses a mass of disorder and defects [23].

The morphologies and structures of the above samples were analyzed by SEM and TEM. Fig. 3a shows the typical TEM image of the raw sample before acid treatment, in which octahedra with core–shell structures were observed clearly. The SAED pattern (inset of Fig. 3b) recorded from the corner of one octahedron contains sharp spots and diffused rings. The former could be indexed as (3 1 1) and (0 4 −4) reflections from fcc Fe_3O_4 and the latter could be indexed as graphite (0 0 2), (1 0) and (0 0 4) reflections. The HRTEM image in Fig. 3b further confirms that the structure is constructed by Fe_3O_4 octahedra core and carbon shell.

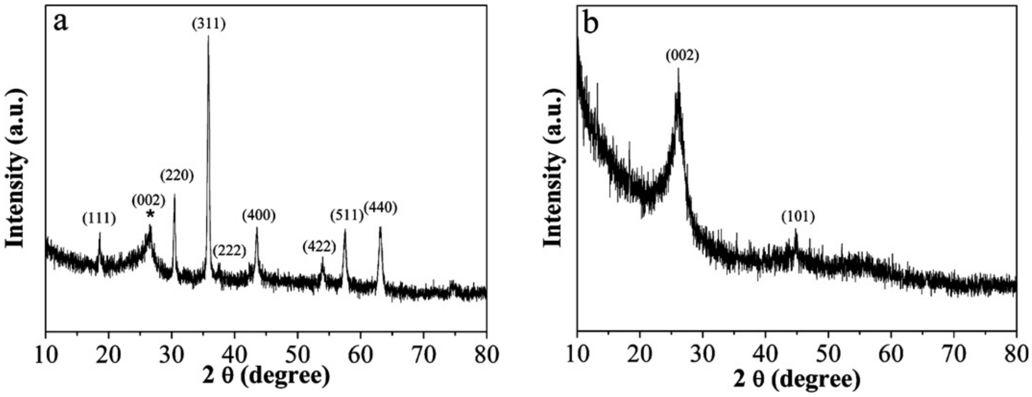

Fig. 1. Typical XRD pattern of the product with the reaction time of 10 h: (a) the raw sample before dilute hydrochloric acid treatment, the diffraction peak marked with * can be indexed to hexagonal graphite (JCPDS Card, No. 41-1487), (b) the as-obtained sample after acid treatment.